Effective Roughness Length for Turbulent Flow over a Wavy Surface

S. J. JACOBS

Department of Atmospheric, Oceanic, and Space Sciences and Department of Mechanical Engineering and Applied Mechanics, The University of Michigan, Ann Arbor, Michigan

(Manuscript received 16 April 1987, in final form 23 November 1988)

ABSTRACT

A two-equation turbulence model is used to calculate the effective roughness length for two-dimensional turbulent flow over small amplitude, wavy surface topography. The governing equations are solved using the method of matched asymptotic expansions for the case $\epsilon \ll 1$, $\delta \ll 1$, where ϵ is the square root of a characteristic drag coefficient for flow over a plane surface and δ is the wave slope. Analytical expressions are derived for the effective roughness length and drag coefficient for flow over stationary topography and over a progressive wave. The results are used to determine the drag coefficient and the form drag for flow over a progressive water wave, and are found to be consistent with observations.

1. Introduction

According to meteorological observations (Garratt 1977), the wind speed for neutrally stratified turbulent flow over an uneven surface can be represented with good accuracy by a logarithmic velocity profile in which the roughness length is given an empirical value depending on the characteristics of the surface topography. Defining the effective surface shear stress as the horizontally averaged streamwise surface force per unit horizontal area and u_τ as the corresponding friction velocity, the velocity profile for flow over surface topography takes the form

$$U = \frac{u_\tau}{\kappa} \ln\left(\frac{x_3}{n_e}\right), \tag{1.1}$$

where U is the horizontally averaged wind speed, x_3 is the vertical distance from the mean surface level, κ is the von Kármán constant, and n_e is the effective roughness length. The drag coefficient C_D relating the effective stress to the wind speed at elevation x_3 is given by

$$C_D = \left(\frac{\kappa}{\ln(x_3/n_e)}\right)^2, \tag{1.2}$$

and increases monotonically with n_e.

In this paper we are concerned with calculating the effective roughness length for two-dimensional turbulent flow over a wavy surface. Because observed roughness lengths for such flows are often several orders of magnitude larger than the intrinsic roughness length, n_0, for flow over a plane surface composed of the same material, the resulting increase in the drag coefficient, shown here in Fig. 1, is significant in the calculation of the wind stress on the sea surface in the presence of water waves (Wu 1980), and in other flows of geophysical interest. The neglect of studies of this effect in the turbulence modeling literature and the practical importance of the problem provide the motivation for the present study.

Our main result can be derived intuitively by considering the momentum balance equation

$$\bar{\tau} + p\overline{\frac{\partial h}{\partial x_1}} = \tau_0, \tag{1.3}$$

in which $\tau_0 = \rho(u_\tau)^2$ is the stress corresponding to u_τ, h is the surface elevation, p and τ are the pressure and the x_1 component of the surface shear stress, respectively, and the overbar denotes a horizontal average. Using this equation, defining the form drag coefficient by

$$C_p = \frac{\overline{p(\partial h/\partial x_1)}}{\rho(u_\tau)^2} \tag{1.4}$$

and assuming that C_p is small, we find that the friction velocity at the surface is given approximately by

$$\left(\frac{\bar{\tau}}{\rho}\right)^{1/2} \approx u_\tau\left[1 - \frac{1}{2}C_p\right]. \tag{1.5}$$

Now defining n_0 as the intrinsic roughness length and assuming that the velocity profile $U(x_3)$ is given by a logarithmic law in which the roughness length is taken as n_0 and the friction velocity as its surface value, it follows from (1.5) that

Corresponding author address: Dr. Stanley Jacobs, Dept. of Atmos., Oceanic, & Space Sciences, 2212 Space Research, The University of Michigan, Ann Arbor, MI 48109.

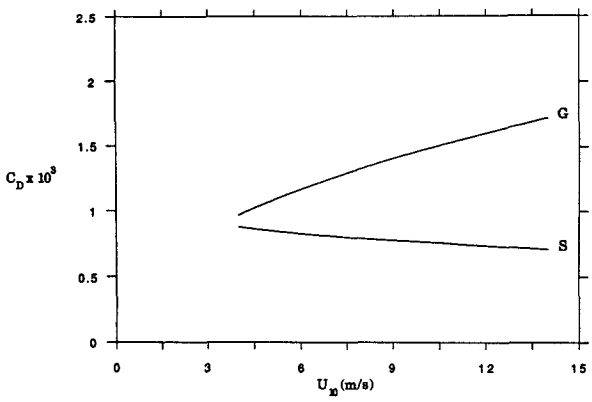

FIG. 1. C_D for elevation 10 m as function of velocity U_{10} for flow over wind waves. Curve G from Garratt's data compilation, curve S for flow over an aerodynamically smooth surface.

$$U(x_3) \approx \frac{u_\tau}{\kappa}\left\{\ln\left(\frac{x_3}{n_0}\right) - \frac{1}{2} C_p \ln\left(\frac{x_3}{n_0}\right)\right\}, \quad (1.6)$$

in which the second term in the brackets is a small correction. To the accuracy of this approximation the logarithm multiplying C_p can be evaluated at some representative elevation, say at $x_3 = L$, where $1/L$ is the wavenumber for a monochromatic wave, and comparing the result of this last approximation with (1.1) suggests that the effective roughness length, n_e, satisfies

$$\ln\left(\frac{n_e}{n_0}\right) = \frac{1}{2} C_p \ln\left(\frac{L}{n_0}\right). \quad (1.7)$$

In the present study our aim is to verify this derivation by a formal analysis, to calculate the form drag coefficient C_p as a function of the parameters, and to use (1.7) to determine the effective roughness length.

In studies of turbulent flow over aerodynamically rough surfaces (Perry et al. 1969), the form drag is caused primarily by boundary layer separation at the top of the roughness elements. This may also be true for flow over water waves, as suggested by Wu. However, experiments by Zilker et al. (1977) on nonseparated flow over a smooth wavy surface show that about 25% of the horizontal force on the surface is associated with form drag, which agrees closely with values quoted for flow over wind-driven waves (Phillips 1977, pp. 189–191). In view of this result, it seems reasonable to investigate the possibility that form drag due to nonseparated flow is the major cause of the large effective roughness lengths observed for turbulent flow over water waves.

Carrying out an investigation of this type necessarily requires the use of a turbulence model to obtain a closed set of equations for the Reynolds averaged velocity and pressure. The present study is based on the use of an eddy viscosity model, as in previous treatments of flow over rigid surface topography (Jackson and Hunt 1975; Taylor et al. 1976; Thorsness et al. 1978; McLean 1983; Beljaars et al. 1987), over water waves (Gent and Taylor 1976; Knight 1977; Al-Zanaidy and Hui 1984; Jacobs 1987), and under water waves (Dvoryaninov and Zhuravlev 1980). In the calculation reported below we employ the two-equation turbulence model of Launder and Spalding, as amended by Singhal and Spalding (1981). This is at least as accurate as the one-equation models used in most previous work on the subject, and in any event the asymptotic analysis of our earlier paper and the numerical calculations of Beljaars et al. indicate that the choice of eddy viscosity model is not crucial to our main results. Studies by Sykes (1980) and Newley (1985) based on the use of second-order closure theory will be discussed later in the paper.

In the following sections the equations of the Launder–Spalding model are treated by expanding the dependent variables in powers of the wave slope for flow over small amplitude topography. The theory is mathematically complicated but conceptually simple; the lowest order term in the expansion of the x_1 component of the Reynolds averaged velocity is a basic solution U_0 for flow over a plane surface, the next term is a sinusoidal correction to the basic flow, and the quadratic term is the sum of a second harmonic and a correction to the horizontally averaged velocity, the latter of which is determined explicitly. The resulting horizontally averaged velocity can be approximated by an expression of the form (1.1), and Eq. (1.7) yields a formula for the effective roughness length as a function of the intrinsic roughness length, n_0, the topographic wavenumber, the wave slope, and the friction velocity. The analysis is carried out for steady flow, but is extended to the case of flow over a progressive wave by use of results obtained in our earlier paper.

As an application, the variation of the drag coefficient with wind speed and the fraction of momentum transfer to the water associated with form drag for flow over progressive water waves are calculated and compared with observations. The comparison shows a satisfactory degree of agreement between the results of the calculation and measurements, but indicates that a more complete specification of the energy spectrum of wind waves is needed to verify the theory.

2. Formulation

Consider steady, constant density, two-dimensional turbulent flow in the semi-infinite region $x_3 > h(x_1)$, with $\vec{u}$ and P denoting the Reynolds-averaged velocity and pressure, and $\vec{u}'$ the fluctuating part of the velocity. Letting angle brackets denote the Reynolds average, define the turbulent energy E, the dissipation rate D, and a pressure-like variable p by

$$E = \frac{1}{2}\langle u_k' u_k' \rangle, \quad D = \frac{\mu}{\rho}\left\langle \frac{\partial u_i'}{\partial x_k}\frac{\partial u_i'}{\partial x_k}\right\rangle, \quad (2.1)$$

$$p = P + \rho\left(\frac{2}{3}E - g_k x_k\right), \tag{2.2}$$

where μ, ρ, and g_k are the shear viscosity, the density, and the kth component of the gravitational vector. Then the Reynolds-averaged continuity and momentum equations become

$$\frac{\partial u_k}{\partial x_k} = 0, \tag{2.3}$$

$$u_k \frac{\partial u_i}{\partial x_k} + \frac{1}{\rho}\frac{\partial p}{\partial x_i} = \frac{\partial \tau_{ki}}{\partial x_k}, \tag{2.4}$$

where the viscous force is neglected and where τ_{ik} is defined by

$$\tau_{ik} = \frac{2}{3}E\delta_{ik} - \langle u_i' u_k' \rangle. \tag{2.5}$$

According to the Launder–Spalding turbulence model, τ_{ik} is expressed in the form

$$\tau_{ik} = \nu\left(\frac{\partial u_i}{\partial x_k} + \frac{\partial u_k}{\partial x_i}\right), \tag{2.6}$$

where ν is an eddy viscosity given by

$$\nu = \frac{(\lambda E)^2}{D}, \tag{2.7}$$

and where, for steady flow, E and D satisfy

$$u_k \frac{\partial E}{\partial x_k} = \nu\left(\frac{\partial u_i}{\partial x_k} + \frac{\partial u_k}{\partial x_i}\right)\frac{\partial u_i}{\partial x_k} + \frac{\partial}{\partial x_k}\left(\nu \frac{\partial E}{\partial x_k}\right) - D, \tag{2.8}$$

$$u_k \frac{\partial D}{\partial x_k} = C_1 \lambda^2 E\left(\frac{\partial u_i}{\partial x_k} + \frac{\partial u_k}{\partial x_i}\right)\frac{\partial u_i}{\partial x_k} + \frac{\partial}{\partial x_k}\left(\frac{\nu}{\sigma}\frac{\partial D}{\partial x_k}\right) - C_2\frac{D^2}{E}. \tag{2.9}$$

The constants appearing in the above equations take the values $\lambda = 0.3$, $C_1 = 1.44$, $C_2 = 1.92$, and

$$\sigma = \frac{\kappa^2}{\lambda(C_2 - C_1)} \tag{2.10}$$

in which $\kappa = 0.4$ is von Kármán's constant.

To express the boundary conditions at a rigid surface, we let $n(\vec{x})$ denote the normal distance from the surface to a point $\vec{x}$ in the fluid, n_0 the surface roughness length, and $\vec{t}$ the tangential part of the kinematic surface stress. Then, defining the vector friction velocity $\vec{s}$ by

$$\vec{t} = |\vec{s}|\vec{s}, \tag{2.11}$$

the dependent variables satisfy

$$\vec{u} \to \frac{\vec{s}}{\kappa}\ln\left(\frac{n}{n_0}\right), \quad E \to \frac{|\vec{s}|^2}{\lambda}, \quad D \to \frac{|\vec{s}|^3}{\kappa n}, \tag{2.12}$$

as $n \to 0$. Other boundary conditions depend on the nature of the flow. In the present study we take these as

$$\vec{u} \to \mathbf{e}_1 \frac{u_\tau}{\kappa}\left[\ln\left(\frac{x_3}{n_0}\right) - C\right], \quad E \to \frac{(u_\tau)^2}{\lambda}, \quad D \to \frac{(u_\tau)^3}{\kappa x_3}, \tag{2.13}$$

as $x_3 \to \infty$, where $\mathbf{e}_1$ is the unit vector pointing in the x_1-direction, u_τ is a prescribed constant, and C is a constant to be calculated as part of the solution.

If $h = 0$ the governing equations admit (2.13) as a solution, with $C = 0$ and with $\vec{s} = (u_\tau)\mathbf{e}_1$. To consider flow over small amplitude sinusoidal topography, we express h as $h = \delta L h^*$, where δ is the dimensionless wave slope, treated here as a small parameter, L is the reciprocal of the topographic wave number, and h^* is the dimensionless surface elevation. Then, anticipating that $C = O(\delta^2)$, introducing dimensionless variables by

$$\vec{x} = L\vec{x}^*, \quad \vec{u} = \frac{u_\tau}{\epsilon}\vec{u}^*,$$
$$p = \rho\left(\frac{u_\tau}{\epsilon}\right)^2 p^*, \quad E = \frac{(u_\tau)^2}{\lambda}E^*,$$
$$D = \frac{(u_\tau)^3}{L}D^*, \quad \nu = Lu_\tau\nu^*,$$
$$\vec{s} = u_\tau\vec{s}^*, \quad C = \delta^2 C^*, \tag{2.14}$$

and omitting the asterisks, we obtain the dimensionless equations

$$\frac{\partial u_k}{\partial x_k} = 0, \tag{2.15}$$

$$u_k\frac{\partial u_i}{\partial x_k} + \frac{\partial p}{\partial x_i} = \epsilon\frac{\partial}{\partial x_k}\left[\nu\left(\frac{\partial u_i}{\partial x_k} + \frac{\partial u_k}{\partial x_i}\right)\right], \tag{2.16}$$

$$u_k\frac{\partial E}{\partial x_k} = \frac{\lambda\nu}{\epsilon}\left(\frac{\partial u_i}{\partial x_k} + \frac{\partial u_k}{\partial x_i}\right)\frac{\partial u_i}{\partial x_k} + \epsilon\frac{\partial}{\partial x_k}\left(\nu\frac{\partial E}{\partial x_k}\right) - \epsilon\lambda D, \tag{2.17}$$

$$u_k\frac{\partial D}{\partial x_k} = \frac{C_1\lambda E}{\epsilon}\left(\frac{\partial u_i}{\partial x_k} + \frac{\partial u_k}{\partial x_i}\right)\frac{\partial u_i}{\partial x_k} + \frac{\epsilon}{\sigma}\frac{\partial}{\partial x_k}\left(\nu\frac{\partial D}{\partial x_k}\right) - \epsilon\lambda C_2\frac{D^2}{E}, \tag{2.18}$$

where the dimensionless eddy viscosity is given by

$$\nu = \frac{E^2}{D}, \tag{2.19}$$

and where

$$\epsilon = \frac{\kappa}{\ln(L/n_0)}. \tag{2.20}$$

The boundary conditions are

$$\vec{u} \to \vec{s}\left[1 + \frac{\epsilon}{\kappa}\ln(n)\right], \quad E \to |\vec{s}|^2, \quad D \to \frac{|\vec{s}|^3}{\kappa n}, \tag{2.21}$$

as $x_3 \to \delta h$, and

$$\vec{u} \to \mathbf{e}_1\left\{1 + \frac{\epsilon}{\kappa}[\ln(x_3) - \delta^2 C]\right\}, \quad E \to 1, \quad D \to \frac{1}{\kappa x_3}, \tag{2.22}$$

as $x_3 \to \infty$.

To complete the formulation, we note that the dependent variables are periodic in x_1 with period 2π, and that $\vec{s}$ takes the form

$$\vec{s} = s\frac{\mathbf{e}_1 + \delta(dh/dx_1)\mathbf{e}_3}{[1 + \delta^2(dh/dx_1)^2]^{1/2}}. \tag{2.23}$$

Using (2.23), integrating the x_1-component of the momentum equation over the area $0 \leqslant x_1 \leqslant 2\pi$, $\delta h \leqslant x_3 \leqslant H$, where H is large, and applying the boundary conditions (2.21) and (2.22), we find that

$$\frac{\delta}{\epsilon^2}\int_0^{2\pi} p\frac{dh}{dx_1}dx_1 + \int_0^{2\pi} s^2 dx_1 = 2\pi, \tag{2.24}$$

which can be recognized as the dimensionless version of (1.3). We note also that if the velocity far from the surface is expressed in the form (1.1), the effective surface roughness is given by

$$n_e = n_0 \exp(\delta^2 C). \tag{2.25}$$

The simplest method of treating the above equations when $\delta \ll 1$ is to expand the solution in the form

$$F = F^{(0)}(\vec{x}) + \delta F^{(1)}(\vec{x}) + \delta^2 F^{(2)}(\vec{x}) + \cdots, \tag{2.26}$$

where F stands for any of the dependent variables, and to transfer the boundary conditions at $x_3 = \delta h$ to the mean surface level, $x_3 = 0$. As noted by Joseph (1973) in another context, the transfer of boundary conditions is often invalid because the field variables cannot be continued analytically outside their domain of definition. Therefore, we follow Joseph by introducing a change of independent variables of the form

$$\vec{x} = \vec{y} + \delta\vec{\phi}(\vec{y}) + \delta^2\vec{\theta}(\vec{y}) + \cdots, \tag{2.27}$$

where the new coordinates are chosen so that the boundary has a simple shape in $\vec{y}$-space, thus allowing (2.21) to be applied at the exact location of the boundary.

Substituting (2.27) into (2.26) and rearranging terms yields

$$F = F^{(0)}(\vec{y}) + \delta\left[F^{(1)}(\vec{y}) + \phi_k\frac{\partial F^{(0)}}{\partial y_k}\right] + \delta^2\left[F^{(2)}(\vec{y}) + \phi_k\frac{\partial F^{(1)}}{\partial y_k} + \theta_k\frac{\partial F^{(0)}}{\partial y_k} + \frac{1}{2}\phi_i\phi_k\frac{\partial^2 F^{(0)}}{\partial y_i \partial y_k}\right] + \cdots, \tag{2.28}$$

and the boundary conditions are satisfied by substituting (2.28) into (2.21). It is shown in Joseph's paper that the partial differential equations satisfied by $F^{(k)}(\vec{y})$ have the same form in $\vec{y}$-space as the equations in $\vec{x}$-space obtained by substituting (2.26) into the original field equations, and the solution for F as a function of $\vec{x}$ is obtained by solving for the terms $F^{(k)}(\vec{y})$ and using the same functional forms for $F^{(k)}(\vec{x})$ in (2.26).

In carrying out this procedure it is convenient to define the new coordinates as (x, z), where

$$x_1 = x - \frac{\delta(dh/x)z}{[1 + \delta^2(dh/dx)^2]^{1/2}}, \quad x_3 = \delta h + \frac{z}{[1 + \delta^2(dh/dx)^2]^{1/2}}, \tag{2.29}$$

so that $x = x_1$ on the boundary, and $z = n$, the normal distance from the boundary to a point in the fluid. The leading term in the expansion (2.28) is a function of z, where, letting u and w denote the velocity components in the x_1 and x_3 directions,

$$u^{(0)} = 1 + \frac{\epsilon}{\kappa}\ln(z) \equiv U(z), \quad w^{(0)} = 0, \quad p^{(0)} = 0, \quad E^{(0)} = 1, \quad D^{(0)} = \frac{1}{\kappa z}, \quad \nu^{(0)} = \kappa z, \quad s^{(0)} = 1. \tag{2.30}$$

Hence, (2.28) takes the form

$$F = F^{(0)}(z) + \delta\left[F^{(1)}(x, z) + h\frac{dF^{(0)}}{dz}\right] + \delta^2\left[F^{(2)}(x, z) - z\frac{dh}{dx}\frac{\partial F^{(1)}}{\partial x} + h\frac{\partial F^{(1)}}{\partial z} - \frac{1}{2}z\left(\frac{dh}{dx}\right)^2\frac{dF^{(0)}}{dz} + \frac{1}{2}h^2\frac{d^2F^{(0)}}{dz^2}\right], \tag{2.31}$$

with an $O(\delta^3)$ error, and the coefficients $\nu^{(k)}$ in the expansion of the eddy viscosity are given by

$$\nu^{(0)} = \kappa z, \quad \nu^{(1)} = 2\kappa z E^{(1)} - (\kappa z)^2 D^{(1)}, \quad \nu^{(2)} = \kappa z[2E^{(2)} + (E^{(1)})^2] - (\kappa z)^2[2E^{(1)}D^{(1)} + D^{(2)}] + (\kappa z)^3(D^{(1)})^3. \tag{2.32}$$

Using (2.32) and defining ∇^2 by

$$\nabla^2 = \frac{\partial^2}{\partial x^2} + \frac{\partial^2}{\partial z^2}, \tag{2.33}$$

the $O(\delta)$ equations are given by

$$\frac{\partial u^{(1)}}{\partial x} + \frac{\partial w^{(1)}}{\partial z} = 0, \tag{2.34}$$

$$U\frac{\partial u^{(1)}}{\partial x} + \frac{\epsilon w^{(1)}}{\kappa z} + \frac{\partial p^{(1)}}{\partial x} = \epsilon\left[\kappa z\nabla^2 u^{(1)} + \kappa\left(\frac{\partial u^{(1)}}{\partial z} + \frac{\partial w^{(1)}}{\partial x}\right)\right] + \epsilon^2\frac{\partial}{\partial z}[2E^{(1)} - \kappa z D^{(1)}], \tag{2.35}$$

$$U\frac{\partial w^{(1)}}{\partial x} + \frac{\partial p^{(1)}}{\partial z} = \epsilon\left[\kappa z\nabla^2 w^{(1)} + 2\kappa\frac{\partial w^{(1)}}{\partial z}\right] + \epsilon^2\frac{\partial}{\partial x}[2E^{(1)} - \kappa z D^{(1)}], \tag{2.36}$$

$$U\frac{\partial E^{(1)}}{\partial x} = \lambda\left[2\left(\frac{\partial u^{(1)}}{\partial z} + \frac{\partial w^{(1)}}{\partial x}\right) + 2\epsilon\left(\frac{E^{(1)}}{\kappa z} - D^{(1)}\right)\right] + \epsilon\left[\kappa z\nabla^2 E^{(1)} + \kappa\frac{\partial E^{(1)}}{\partial z}\right], \tag{2.37}$$

$$U\frac{\partial D^{(1)}}{\partial x} - \frac{w^{(1)}}{\kappa z} = \lambda\left\{\frac{2C_1}{\kappa z}\left(\frac{\partial u^{(1)}}{\partial z} + \frac{\partial w^{(1)}}{\partial x}\right) + \frac{\epsilon}{\kappa z}\left[(C_1 + C_2)\frac{E^{(1)}}{\kappa z} - 2C_2 D^{(1)}\right]\right\} + \frac{\epsilon}{\sigma}\left[\kappa z\nabla^2 D^{(1)} + 2\kappa\frac{\partial}{\partial z}\left(D^{(1)} - \frac{E^{(1)}}{\kappa z}\right)\right], \tag{2.38}$$

with boundary conditions

$$u^{(1)} \to s^{(1)}\left[1 + \frac{\epsilon}{\kappa}\ln(z)\right] - \frac{\epsilon h}{\kappa z}, \quad w^{(1)} \to \frac{dh}{dx}\left[1 + \frac{\epsilon}{\kappa}\ln(z)\right], \quad E^{(1)} \to 2s^{(1)}, \quad D^{(1)} \to \frac{3s^{(1)}}{\kappa z} + \frac{h}{\kappa z^2}, \tag{2.39}$$

as $z \to 0$, and

$$u^{(1)} \to 0, \quad w^{(1)} \to 0, \quad E^{(1)} \to 0, \quad D^{(1)} \to 0, \tag{2.40}$$

as $z \to \infty$. It can also be shown using (2.24) that

$$\overline{s^{(1)}} = 0, \tag{2.41}$$

where the overbar denotes the horizontal average.

The formulation of the $O(\delta^2)$ problem is lengthy, and we quote only the equations needed to determine the topographically induced correction to the horizontally averaged x_1-component of $\vec{u}$. These are the horizontal averages of the x_1-momentum equation and of the boundary conditions on u, and are given by

$$\overline{u^{(1)}w^{(1)}} = \epsilon\left[\kappa z\frac{\partial}{\partial z}\overline{u^{(2)}} + \overline{\nu^{(1)}\left(\frac{\partial u^{(1)}}{\partial z} + \frac{\partial w^{(1)}}{\partial x}\right)} + \frac{\epsilon}{\kappa z}\overline{\nu^{(2)}}\right], \tag{2.42}$$

$$\overline{u^{(2)}} = \bar{Q} \tag{2.43}$$

at $z = 0$, and

$$\overline{u^{(2)}} \to -\frac{\epsilon C}{\kappa} \tag{2.44}$$

as $z \to \infty$, where

$$Q = \lim_{z\to 0}\left\{z\frac{dh}{dx}\frac{\partial u^{(1)}}{\partial x} - h\frac{\partial u^{(1)}}{\partial z} + \frac{\epsilon}{2\kappa}\left[\left(\frac{dh}{dx}\right)^2 + \left(\frac{h}{z}\right)^2\right] + \left[s^{(2)} - \frac{1}{2}\left(\frac{dh}{dx}\right)^2\right] \times\left[1 + \frac{\epsilon}{\kappa}\ln(z)\right]\right\}. \tag{2.45}$$

We also need the $O(\delta^2)$ contribution to (2.24),

$$\overline{(s^{(1)})^2 + 2s^{(2)}} = -\frac{1}{\epsilon^2}\overline{p^{(1)}\frac{dh}{dx}}. \tag{2.46}$$

As in our earlier paper, we consider the case $\epsilon \ll 1$, which holds for all wavenumbers $(1/L)$ satisfying $n_0 \ll L$, and we treat the above equations using the method of matched asymptotic expansions.

3. Solution of the $O(\delta)$ equations

We consider now flow over sinusoidal topography described by $h = \cos(x)$, and we omit the superscripts in writing the dependent variables for the $O(\delta)$ problem.

As the small parameter ϵ multiplies the most highly differentiated terms in the $O(\delta)$ momentum equations, the flow has a boundary layer structure consisting of an outer solution valid for $z = O(1)$ and an inner solution with dimensionless length scale ϵ which holds near the boundary. The solution for u, w, p, and E in each region takes the form

$$u = \{u^{[0]}\} + \{\epsilon\ln(\epsilon)u^{[1]} + \epsilon u^{[2]}\} + \cdots, \tag{3.1}$$

while the solution for D is of the form (3.1) in the outer region but involves terms $O(1/\epsilon)$ and $O(1/\epsilon^2)$ in the inner region. In the following calculation u, w, and p will be computed to the order shown in (3.1), while E and D will be determined to lowest order. For purposes of matching, each bracketed expression in

(3.1) must be treated as a single term (cf. Van Dyke 1975, p. 221).

Turning first to the outer problem, we express u and w in terms of a streamfunction, ψ, through

$$u = -\frac{\partial \psi}{\partial z}, \quad w = \frac{\partial \psi}{\partial x}, \tag{3.2}$$

and expand ψ, p, E, and D in the form (3.1). It follows that $\psi^{[k]}$ satisfies Laplace's equation for $k = 0, 1$, that

$$p^{[k]} = \frac{\partial \psi^{[k]}}{\partial z}, \quad E^{[k]} = 4\lambda \frac{\partial \psi^{[k]}}{\partial x},$$
$$D^{[k]} = \frac{4\lambda C_1}{\kappa z} \frac{\partial \psi^{[k]}}{\partial x} + \frac{\psi^{[k]}}{\kappa z^2}, \tag{3.3}$$

again for $k = 0, 1$, that $\psi^{[2]}$ is the solution of

$$\nabla^2 \psi^{[2]} = -\frac{\psi^{[0]}}{\kappa z^2}, \tag{3.4}$$

and that

$$p^{[2]} = \frac{\partial \psi^{[2]}}{\partial z} + 2\kappa \frac{\partial \psi^{[0]}}{\partial x} + \frac{\ln(z)}{\kappa} \frac{\partial \psi^{[0]}}{\partial z} - \frac{\psi^{[0]}}{\kappa z}. \tag{3.5}$$

For the surface elevation $h = \cos(x)$, the solution for $\psi^{[k]}$ satisfying the boundary condition $\psi^{[k]} \to 0$ as $z \to \infty$ is

$$\psi^{[0]} = A^{[0]} \cos(x) e^{-z}, \quad \psi^{[1]} = A^{[1]} \cos(x) e^{-z},$$
$$\psi^{[2]} = A^{[2]} \cos(x) e^{-z} - \cos(x) \frac{A^{[0]}}{\kappa} e^z E_1(2z), \tag{3.6}$$

where

$$E_1(z) = \int_z^\infty \frac{e^{-t}}{t}\, dt \tag{3.7}$$

is the exponential integral (Olver 1974, p. 40), with small argument expansion

$$E_1(z) = -\ln(z) - \gamma + \sum_{n=1}^{\infty} \frac{(-1)^{n-1}}{n} \frac{z^n}{n!}, \tag{3.8}$$

in which $\gamma = 0.57722$ is Euler's constant.

Matching with the inner solution discussed below yields

$$A^{[0]} = 1, \quad A^{[1]} = 0, \quad A^{[2]} = -\frac{\gamma + \ln(2)}{\kappa}, \tag{3.9}$$

and hence, in the outer region,

$$u = \cos(x) e^{-z} + \frac{\epsilon}{\kappa} \cos(x) \left[e^z E_1(2z) - \frac{e^{-z}}{z} - (\gamma + \ln(2)) e^{-z} \right], \tag{3.10}$$

$$w = -\sin(x) e^{-z} + \frac{\epsilon}{\kappa} \sin(x) [e^z E_1(2z) + (\gamma + \ln(2)) e^{-z}], \tag{3.11}$$

$$p = -\cos(x) e^{-z} - 2\kappa\epsilon \sin(x) e^{-z} - \frac{\epsilon}{\kappa} \cos(x) \times [e^z E_1(2z) + \ln(z) e^{-z} - (\gamma + \ln(2)) e^{-z}], \tag{3.12}$$

with an error $O[\epsilon^2 \ln(\epsilon)]$, and

$$E = -4\lambda \sin(x) e^{-z},$$
$$D = \left[\frac{1}{\kappa z^2} \cos(x) - \frac{4\lambda C_1}{\kappa z} \sin(x) \right] e^{-z} \tag{3.13}$$

with an error $O[\epsilon \ln(\epsilon)]$.

In treating the inner equations we define a stretched boundary layer coordinate $\zeta = z/\epsilon$ and introduce the variables $Q_x, Q_z, \hat{p}, \hat{E}$, and $\hat{D}$ through

$$u = Q_x - \frac{h}{\kappa \zeta}, \quad w = \frac{dh}{dx} U + \epsilon Q_z, \quad p = \hat{p},$$
$$E = \hat{E}, \quad D = \frac{h}{\kappa \epsilon^2 \zeta^2} + \frac{1}{\epsilon} \hat{D}. \tag{3.14}$$

Since

$$U = 1 + \frac{\epsilon}{\kappa} [\ln(\epsilon) + \ln(\zeta)] \tag{3.15}$$

in the inner region, the boundary conditions are expressed in terms of these variables by

$$\hat{u} \to s^{[0]} + \epsilon \ln(\epsilon) \left[s^{[1]} + \frac{s^{[0]}}{\kappa} \right] + \epsilon \left[s^{[2]} + \frac{s^{[0]}}{\kappa} \ln(\zeta) \right],$$
$$\hat{w} \to 0, \quad \hat{E} \to 2s^{[0]}, \quad \hat{D} \to \frac{3}{\kappa \zeta} s^{[0]}, \tag{3.16}$$

as $\zeta \to 0$, where the boundary conditions on E and D are given only to lowest order. The matching conditions will be stated later, and the equations needed to determine the inner solution to lowest order for $\hat{E}$ and $\hat{D}$ and up to and including $O(\epsilon)$ terms for Q_x, Q_z, and $\hat{p}$ are

$$\frac{\partial Q_x}{\partial x} + \frac{\partial Q_z}{\partial \zeta} = 0, \tag{3.17}$$

$$U \frac{\partial Q_x}{\partial x} + \frac{\epsilon}{\kappa \zeta} Q_z + \frac{\partial \hat{p}}{\partial x} = \kappa \left[\frac{\partial}{\partial \zeta} \left(\zeta \frac{\partial Q_x}{\partial \zeta} \right) + \epsilon \frac{d^2 h}{dx^2} \right] + \epsilon \frac{\partial}{\partial \zeta} [2\hat{E} - \kappa \zeta \hat{D}], \tag{3.18}$$

$$\frac{\partial \hat{p}}{\partial \zeta} = -\epsilon \frac{d^2 h}{dx^2}, \tag{3.19}$$

$$\frac{\partial \hat{E}}{\partial x} = 2\lambda\left[\frac{1}{\epsilon}\frac{\partial Q_x}{\partial \zeta} + \frac{\hat{E}}{\kappa\zeta} - \hat{D} + \frac{d^2h}{dx^2}\right] + \kappa\frac{\partial}{\partial\zeta}\left(\zeta\frac{\partial \hat{E}}{\partial\zeta}\right), \tag{3.20}$$

$$\frac{\partial \hat{D}}{\partial x} - \frac{Q_z}{\kappa\zeta^2} = \frac{2\lambda C_1}{\kappa\zeta}\left[\frac{1}{\epsilon}\frac{\partial Q_x}{\partial\zeta} + \frac{d^2h}{dx^2}\right] + \frac{\lambda}{\kappa\zeta}\left[(C_1 + C_2)\frac{\hat{E}}{\kappa\zeta} - 2C_2\hat{D}\right] + \frac{\kappa}{\sigma}\left[\zeta\frac{\partial^2\hat{D}}{\partial\zeta^2} + 2\frac{\partial}{\partial\zeta}\left(\hat{D} - \frac{\hat{E}}{\kappa\zeta}\right)\right]. \tag{3.21}$$

It can be seen by inspection that the O(1) and O[$\epsilon\ln(\epsilon)$] contributions to Q_x and p are independent of ζ, and so these quantities can be determined by matching with the outer solution. The boundary conditions and (3.17) then provide the corresponding contributions to s and Q_z. Carrying out the calculation to O(ϵ) yields the inner solution for the original variables in the form

$$u = \cos(x)\left\{1 - \frac{1}{\kappa\zeta} - \frac{\epsilon\ln(\epsilon)}{\kappa} + \frac{\epsilon}{\kappa}[1 - 2\gamma - 2\ln(2) - \kappa\zeta - \ln(\zeta)]\right\} + \epsilon\hat{u}(x,\zeta), \tag{3.22}$$

$$w = \sin(x)\left\{-1 - \frac{\epsilon\ln(\epsilon)}{\kappa} + \epsilon\left(\zeta - \frac{\ln(\zeta)}{\kappa}\right)\right\}, \tag{3.23}$$

$$p = -\cos(x) + \epsilon\left\{\cos(x)\left[\zeta + \frac{2}{\kappa}(\gamma + \ln(2))\right] - 2\kappa\sin(x)\right\}, \tag{3.24}$$

$$E = \hat{E}(x,\zeta), \quad D = \frac{\cos(x)}{\epsilon^2\kappa\zeta^2} + \frac{1}{\epsilon}\hat{D}(x,\zeta), \tag{3.25}$$

$$s = \cos(x)\left\{1 - \frac{2\epsilon\ln(\epsilon)}{\kappa}\right\} + \epsilon\hat{s}(x), \tag{3.26}$$

where $\hat{u}$, $\hat{E}$, $\hat{D}$, and $\hat{s}$ remain to be determined.

These quantities are computed by substituting (3.22)–(3.26) into the field equations, the boundary conditions, and the matching conditions to obtain the system

$$\frac{\partial\hat{u}}{\partial x} = \frac{\partial}{\partial\zeta}\left(\kappa\zeta\frac{\partial\hat{u}}{\partial\zeta}\right) + \frac{\partial}{\partial\zeta}(2\hat{E} - \kappa\zeta\hat{D}), \tag{3.27}$$

$$\frac{\partial\hat{E}}{\partial x} = \frac{\partial}{\partial\zeta}\left(\kappa\zeta\frac{\partial\hat{E}}{\partial\zeta}\right) + 2\lambda\left[\frac{\partial\hat{u}}{\partial\zeta} + \frac{\hat{E}}{\kappa\zeta} - \hat{D} - \left(2 + \frac{1}{\kappa\zeta}\right)\cos(x)\right], \tag{3.28}$$

$$\frac{\partial\hat{D}}{\partial x} = \frac{\sin(x)}{\kappa\zeta} + \frac{\kappa}{\sigma}\left[\zeta\frac{\partial^2\hat{D}}{\partial\zeta^2} + 2\frac{\partial}{\partial\zeta}\left(\hat{D} - \frac{\hat{E}}{\kappa\zeta}\right)\right] + \frac{\lambda}{\kappa\zeta}\left[(C_1 + C_2)\frac{\hat{E}}{\kappa\zeta} - 2C_2\hat{D}\right] + \frac{2\lambda C_1}{\kappa\zeta}\left[\frac{\partial\hat{u}}{\partial\zeta} - \left(2 + \frac{1}{\kappa\zeta}\right)\cos(x)\right], \tag{3.29}$$

with boundary conditions

$$\frac{\partial\hat{u}}{\partial\zeta} \to \frac{2}{\kappa\zeta}\cos(x), \quad \hat{E} \to 2\cos(x), \quad \hat{D} \to \frac{3}{\kappa\zeta}\cos(x), \tag{3.30}$$

as $\zeta \to 0$, and matching conditions

$$\hat{u} \to 0, \quad \hat{E} \to -4\lambda\sin(x), \quad \hat{D} \to -[\cos(x) + 4\lambda C_1\sin(x)]/\kappa\zeta, \tag{3.31}$$

as $\zeta \to \infty$. The O(ϵ) contribution to s is given by

$$\hat{s} = \lim_{\zeta\to 0}\left\{\hat{u} - \frac{\cos(x)}{\kappa}[2\ln(2\zeta) + 2\gamma - 1]\right\}. \tag{3.32}$$

Before presenting the solution to this system, we note that the main result of the analysis given above is the expression (3.24) for the pressure in the inner region, since this can be used to determine the form drag $p(dh/dx)$ discussed earlier. Furthermore, as shown in our earlier paper, the same result for the form drag is obtained using any eddy viscosity model for which the eddy viscosity tends to $\kappa|\vec{s}|n$ as $n \to 0$, where $\vec{s}$ is the vector friction velocity.

To solve the system (3.27)–(3.31) we define $Z = \ln(\zeta)$ as a new independent variable and express $\hat{u}$ in the form

$$\hat{u} = F(Z)\cos(x) + G(Z)\sin(x) \tag{3.33}$$

with a similar decomposition for $\hat{E}$, $\hat{D}$, and $\hat{s}$. Then the problem can be expressed as a system of first-order differential equations of the general form

$$\frac{d\mathbf{w}}{dZ} = \vec{H}(\mathbf{w}, Z), \quad a < Z < b \tag{3.34}$$

with boundary conditions

$$\vec{L}(\mathbf{w}) = 0 \quad \text{at} \quad Z = a, \quad \vec{R}(\mathbf{w}) = 0 \quad \text{at} \quad Z = b, \tag{3.35}$$

where $\mathbf{w}$ is the state vector.

If (3.34) is approximated using the implicit midpoint rule and if Z_k and W_{ik} are defined as the grid points and the matrix $w_i(Z_k)$, respectively, then the system (3.34)–(3.35) is replaced by the algebraic system $\vec{S}(\vec{W}) = 0$. Similarly, a pseudospectral approximation to (3.34)–(3.35) yields the algebraic system $\vec{T}(\vec{W})$

$= 0$. The algebraic system obtained using the implicit midpoint rule can be solved efficiently by Newton iteration because the Jacobian matrix for $\vec{S}$ has a narrow bandwidth, while the much more accurate pseudospectral solution is difficult to compute because the Jacobian matrix for $\vec{T}$ is dense.

In order to obtain spectral accuracy at a comparatively low computational cost, we express the equation $\vec{T}(\vec{W}) = 0$ in the form

$$\vec{S}(\vec{W}) = \vec{S}(\vec{W}) - \vec{T}(\vec{W}), \tag{3.36}$$

and solve (3.36) iteratively using the defect correction scheme

$$\vec{S}(\vec{W}_0) = 0, \quad \vec{S}(\vec{W}_{n+1}) = \vec{S}(\vec{W}_n) - \vec{T}(\vec{W}_n), \quad n = 0, 1, \cdots, \tag{3.37}$$

in which $\vec{W}_n$ for $n \geq 0$ is calculated using Newton iteration. As noted by the author (Jacobs 1989), the iteration (3.37) converges rapidly, and its accuracy can be monitored by calculating the spectral coefficients in an expansion of $\mathbf{w}$ in Chebyshev polynomials and by increasing the number of grid points until the coefficients of the highest order Chebyshev polynomials are sufficiently small.

The present calculation was carried out using 65 grid points, with end points $Z = -9$, corresponding to $\zeta = 1.234 \times 10^{-4}$, and $Z = 3$, for which $\zeta = 20.086$. Although the solution for F and G as shown in Figs. 2 and 3 is not in close agreement with the results obtained in our earlier paper using the simple eddy viscosity model $\nu = \kappa|\vec{s}|n$, the expressions obtained here and in our earlier paper for the pressure are identical.

The quantity p_s, defined here as the surface pressure nondimensionalized using $\rho(u_\tau)^2$, can be compared with numerical results obtained by Taylor et al. using a one-equation turbulence model. Their model is nonlinear, and so we limit our comparison to the smallest values of the wave slope given in their Table 1. The flow treated in their study corresponds in the present notation to the case $\epsilon = 0.056$. The comparison is shown in our Table 1, in which J refers to our results and T to those of Taylor et al., and where the phase is defined by writing p_s in the form

$$A + B\cos(x - \text{phase}).$$

As expected, the present results agree well with those of Taylor et al. for small values of δ, but are less accurate for larger slopes.

The form drag for the surface pressure (3.24) is given in terms of our original scaling by

$$\overline{p\frac{dh}{dx}} = \epsilon\kappa, \tag{3.38}$$

which, when substituted into (2.46), yields the solution for the $O(\delta^2)$ contribution to the horizontally averaged friction velocity in the form

$$\overline{s^{(2)}} = -\frac{\kappa}{2\epsilon} + O(1). \tag{3.39}$$

This important result can be checked by calculating the dimensionless horizontally averaged surface shear stress,

$$\bar{\tau} = 1 - \frac{\delta^2\kappa}{\epsilon} \tag{3.40}$$

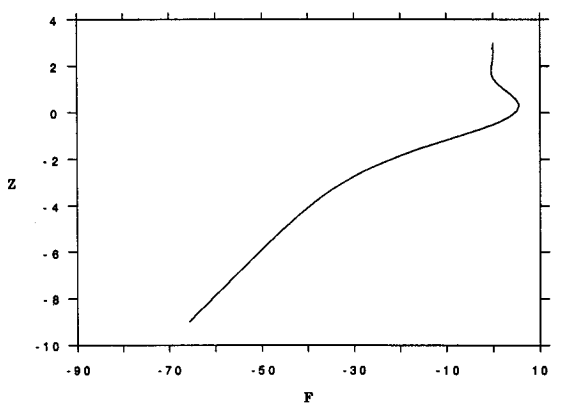

FIG. 2. Function $F(Z)$.

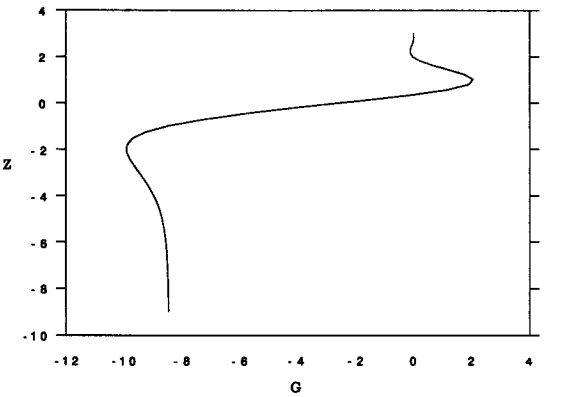

FIG. 3. Function $G(Z)$.

TABLE 1. Amplitude and phase of p_s as function of slope δ.

δ	P_{max} (J)	Phase (J) (deg)	P_{max} (T)	Phase (T) (deg)
0.031	6.67	184	6.8	186
0.063	13.38	184	12.6	187
0.094	19.97	184	17.3	189
0.126	16.77	184	20.6	191

TABLE 2. Dimensionless mean shear stress as function of slope δ.

δ	$\bar{\tau}$ (J)	$\bar{\tau}$ (T)
0.031	0.99	0.99
0.063	0.97	0.96
0.094	0.94	0.92
0.126	0.88	0.86

according to the present theory, and comparing the results with those of Taylor et al. for the parameter values used earlier in Table 1. The comparison is given in Table 2, and shows little difference between our results and those of Taylor et al.

Turning now to a comparison of our results with observations, we temporarily express the pressure in dimensional terms and find that the surface pressure is given to lowest order by

$$\frac{p}{\rho(u_\tau)^2} = -\frac{\delta}{\epsilon^2}\cos\left(\frac{x_1}{L}\right), \tag{3.41}$$

and the drag coefficient for form drag by

$$C_p = \frac{\overline{p(dh/dx_1)}}{\rho(u_\tau)^2} = \frac{\delta^2\kappa}{\epsilon}. \tag{3.42}$$

These quantities have been measured by Zilker et al. and Zilker and Hanratty (1979), and computed theoretically in papers cited earlier by Taylor et al. using both a one-equation turbulence model and mixing length theory, by McLean using mixing length theory, by Knight using a two-equation model, by Sykes using the second-order turbulence closure theory of Launder et al. (1975), and, most recently, by Newley using a modified version of this model. As indicated earlier, calculation of the form drag coefficient is necessary in the computation of the wave-induced correction to the mean horizontal flow.

In the experiments the wave length $\Lambda = (2\pi L)$ is 5.08 cm, and, as an extreme test of our theory, we consider the case $\delta = 0.157$. This corresponds to the wave $(2a/\Lambda) = 0.05$ in the experimental papers, for which the boundary layer is on the verge of separating. The observed surface pressure is of the form (3.41) but is larger by a factor 1.242, and the coefficient C_p takes the value 0.206 according to (3.42), and 0.26 according to observations. The present theory is therefore in reasonable quantitative agreement with the measurements of Hanratty and colleagues, but, for this large amplitude wave, the observed form drag is larger than our theoretical result by a factor of about 1.25.

In previous theoretical calculations of the form drag using an eddy viscosity model, Knight obtains the same expression as ours using an asymptotic theory similar to that given here, and finds by a comparison with an older set of experiments that his theory underestimates the form drag by 15%. The same expression for C_p, (3.42), is obtained from an asymptotic analysis of the one-equation model treated by Taylor et al. However, their numerical calculation for the case $\delta = 0.157$, $\epsilon = 0.054$, yields a value of the form drag larger than ours by a factor of about 1.2. Taylor et al. also present results for this case calculated using mixing length theory, and obtain a value for C_p larger than ours by a factor of 1.4. McLean's numerical calculations of the form drag are in good agreement with those of Taylor et al.

As regards the calculation of the form drag by Sykes and by Newley, a sample of their computations of the quantity

$$A = \frac{C_p}{\delta^2} \tag{3.43}$$

is given in Table 3, in which Newley's results are taken from his Table 6.11, the mixing length results in Table 3 are calculated by Newley, and Sykes' results are summarized in Newley's Chapter 6. The runs reported in Table 3 correspond to an amplitude of 20 m, a wavelength of 2000 m, and various intrinsic roughness lengths. Although the values of ϵ for runs X and Y are probably too large for our theory to be accurate, values for A computed using (3.42) are included in Table 3 for the sake of completeness.

Newley also presents a comparison of his results and those obtained using mixing length theory with the measurements of Zilker and Hanratty in his Fig. 6.32. This figure and the values of A in Table 3 suggest that the calculation of the form drag using mixing length theory is in reasonably good agreement with the measurements, but, for small wave slopes, Newley's theory underestimates A as compared to the measurements by about a factor of two and Sykes' theory by a factor of five or six. This is disconcerting because Sykes and Newley present strong theoretical arguments in support of their use of a second-order turbulence model in preference to an eddy viscosity model. The rather large difference between Sykes' analytical and Newley's numerical results for A is equally upsetting because of the close similarity of their turbulence models.

We are unable to provide any good explanation for the latter discrepancy. With regard to the differences

TABLE 3. $A = C_p/\delta^2$. (S) Sykes asymptotic calculation using second order turbulence model; (N) Newley numerical calculation using second order turbulence model; (J) Present theory; (ML) Newley numerical calculation using mixing length theory.

Run	n_0 (cm)	A (S)	A (N)	A (J)	A (ML)
X	30	2.00	6.31	6.96	12.4
Y	10	2.00	6.10	8.07	12.6
Z	3	2.00	5.74	9.27	14.7

between measured values of C_p and the calculations of Sykes and Newley, it should be noted that both authors use a form of the model of Launder et al. in which the wall proximity contribution to the pressure strain term is omitted. Since the resulting approximated equations employed by Sykes and Newley are incompatible with the turbulent law of the wall for equilibrium flow over a plane boundary, this neglect leads to an error in their calculation, the magnitude of which can only be estimated by redoing their analysis.

In view of the above discussion, it appears that for reasons as yet unknown the calculation of the form drag by Sykes and by Newley disagrees with measurements by an unacceptably large amount, and that the present theory underestimates the form drag by about 25%, either because of our neglect of nonlinearity or because higher order terms in the expansion (3.1) are needed to obtain an accurate result. Therefore, we will treat the $O(\delta^2)$ contribution to the mean flow in the next section using the present turbulence model in preference to the model employed by Sykes and Newley, with the understanding that our theory underestimates the form drag and therefore necessarily underestimates the effective roughness length.

4. Calculation of the horizontally averaged flow

In discussing the horizontally averaged flow we revert to the use of superscripts to denote the order of a term in an expansion in powers of δ. The equations needed to determine the topographically induced correction to the averaged horizontal velocity are (2.42)–(2.45), in which, by reference to (3.39) and the boundary condition at $z = 0$, $\overline{u^{(2)}}$ has an $O(\epsilon^{-1})$ contribution. Analysis of (2.42) shows that the term $(\epsilon^2/\kappa z)\overline{\nu^{(2)}}$ is $O(\epsilon)$ in both the inner and outer regions, as is the left side of the equation, while the term involving $\nu^{(1)}$ is given to lowest order by

$$\overline{\epsilon\nu^{(1)}\left(\frac{\partial u^{(1)}}{\partial z}+\frac{\partial w^{(1)}}{\partial x}\right)} = -\frac{1}{2\zeta^2} \tag{4.1}$$

in the inner region and is $O(\epsilon)$ in the outer region.

It follows that the $O(\epsilon^{-1})$ contribution to $u^{(2)}$ is constant in the outer region and satisfies

$$\frac{d}{d\zeta}\overline{u^{(2)}} = \frac{1}{2\epsilon\kappa\zeta^3} \tag{4.2}$$

in the inner region. An analogous analysis of the boundary conditions yields

$$\overline{u^{(2)}} \to -\frac{\kappa}{2\epsilon}-\frac{1}{4\epsilon\kappa\zeta^2} \quad \text{as} \quad \zeta \to 0,$$

$$\overline{u^{(2)}} \to -\frac{\epsilon C}{\kappa} \quad \text{as} \quad \zeta \to \infty, \tag{4.3}$$

and so the composite solution for $\overline{u^{(2)}}$ takes the form

$$\overline{u^{(2)}} = -\frac{\kappa}{2\epsilon}-\frac{\epsilon}{4\kappa z^2}, \tag{4.4}$$

and the constant C is given by

$$C = \frac{\kappa^2}{2\epsilon^2}. \tag{4.5}$$

Restricting our attention now to flow in the outer region, using dimensional variables, and defining U as the horizontally averaged x_1 component of velocity, we find that to lowest order

$$U = \frac{u_\tau}{\kappa}\ln\left(\frac{x_3}{n_e}\right), \tag{4.6}$$

where, substituting (4.5) into (2.25), the effective roughness length is given according to the present theory by

$$n_e = n_0 \exp\left[\Gamma\left(\frac{\delta\kappa}{\epsilon}\right)^2\right], \tag{4.7}$$

in which $\Gamma = \frac{1}{2}$. To extend this result to flow over a monochromatic progressive water wave, we let c denote the phase speed of the wave and use the calculation of the surface pressure given in our earlier paper to find that in this case n_e is given by (4.7) with Γ replaced by

$$\Gamma = \frac{1}{2}\left(1-\frac{\epsilon c}{u_\tau}\right). \tag{4.8}$$

The formula for the effective roughness length can also be expressed in the form

$$\ln\left(\frac{n_e}{n_0}\right) = \frac{1}{2}C_p\ln\left(\frac{L}{n_0}\right), \tag{4.9}$$

derived earlier in the paper, where L is the ratio of the wave length Λ to 2π and where C_p is given for the progressive wave case by

$$C_p = \delta^2\left[\ln\left(\frac{L}{n_0}\right)-\frac{\kappa c}{u_\tau}\right]. \tag{4.10}$$

In the case of flow over progressive water waves, to which we now restrict our attention, we assume that the intrinsic roughness length can be approximated by use of a result for flow over an aerodynamically smooth surface,

$$n_0 = \exp(-5.5\kappa)\frac{\nu_a}{u_\tau}, \tag{4.11}$$

(Schlichting 1979, pp. 616–619), where ν_a is the kinematic viscosity of air. The calculation of the effective

roughness length then reduces to evaluating (4.9) and (4.10). Theoretically, this can be accomplished by redoing the calculation in a form allowing the replacement of the various horizontal averages by spectral averages. In practice, these averages depend strongly on the large frequency tail of the slope spectrum for wind-driven water waves, which is not known with sufficient accuracy for the calculation of reliable results. Accordingly, the method used here to compute the effective roughness length is an approximation in which δ^2 on the right side of (4.10) is replaced by an empirical value for the mean square slope $\overline{\delta^2}$ and the rest of the expression is evaluated at a representative wave frequency.

The value used here for the mean square slope is

$$\overline{\delta^2} = 5.326 \times 10^{-3} U_{10}, \qquad (4.12)$$

(Cox and Munk 1954), where U_{10} is the wind speed in m s^{-1} at 10 m elevation and where (4.12) applies for wind speeds less than about 14 m s^{-1}. The consensus in the literature is that form drag is associated primarily with short waves, for which the frequency is large compared to $\omega = (g/U_{10})$, where U_{10} is the wind speed at 10 m elevation. Evaluation of the logarithm in (4.9) and (4.10) shows it to be relatively constant for values of the frequency in the range ω to 10ω, and we eventually took $1/L$ as the wavenumber corresponding to a frequency 5ω. Although this method is somewhat crude, it has the advantage that it takes the contribution of small-scale waves to the form drag into account through use of the empirical expression (4.12) for the mean square slope. Nevertheless, it would be better if the large frequency behavior of the slope spectrum were known with sufficient accuracy to evaluate the spectral averages discussed above.

In carrying out this procedure, the effective roughness length n_e was eliminated between (4.9) and (1.2)

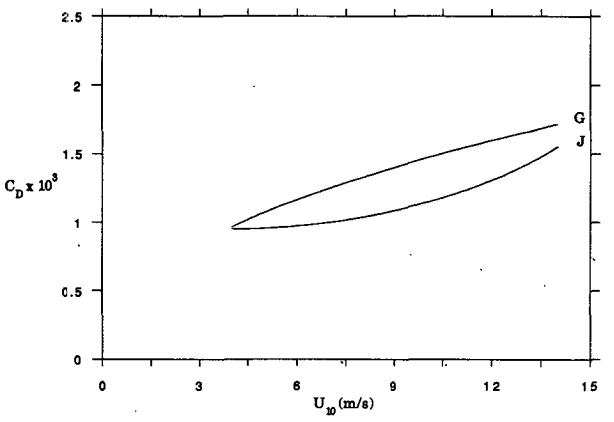

FIG. 4. C_D as function of U_{10}. Curve G from Garratt's data compilation, curve J from present theory.

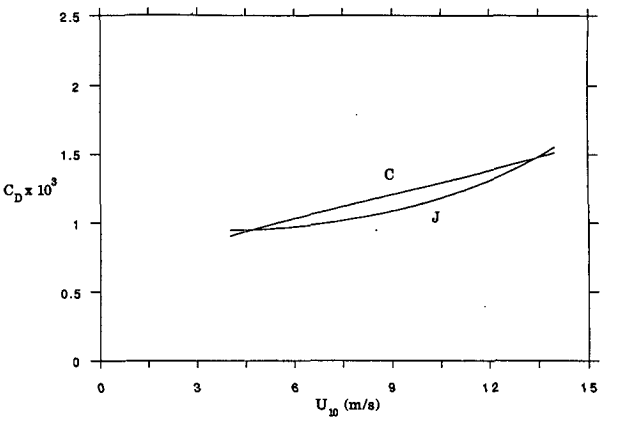

FIG. 5. C_D as function of U_{10}. Curve C from Charnock relation with $\alpha = 0.011$, curve J from present theory.

to obtain a relation $F(C_D, U_{10}) = 0$, where C_D is now defined as the drag coefficient for winds at 10 m elevation. Solving this equation numerically yields C_D as a function of U_{10}, and the effective roughness length can then be calculated as a function of U_{10}.

Empirical relations between the drag coefficient and the wind speed are usually expressed either by fitting the drag coefficient by

$$C_{10} = 10^{-3} A (U_{10})^B, \qquad (4.13)$$

where A and B are constants and U_{10} is given in m s^{-1}, or by assuming a Charnock relation

$$n_e = \alpha \frac{(u_\tau)^2}{g}, \qquad (4.14)$$

where α is the Charnock constant. Wu finds the empirical values $A = 0.5$, $B = 0.5$, $\alpha = 0.0185$, and Garratt suggests the values $A = 0.51$, $B = 0.46$, $\alpha = 0.0144$. The difference between Wu's results and Garratt's is not large, and in Fig. 4 we show a comparison between our values for the drag coefficient and those computed using (4.13) and Garratt's values for A and B. In Fig. 5 we show a comparison of the drag coefficient computed here with the drag coefficient obtained using Charnock's formula, with α given the value 0.011 suggested by Phillips (1977, p. 195).

As can be seen, the present theory is extremely accurate if Phillips' value for the Charnock constant is correct, but is low by as much as 25% as compared to the results of Wu and Garratt. Since our theory for the form drag has been shown earlier to provide an underestimate for this quantity, it appears that our values of C_D are on the low side as compared to measured drag coefficients. However, the drag coefficient data analyzed by Wu and Garratt is too highly scattered to form any firm conclusions on this point.

Another quantity of interest is the pressure drag coefficient given theoretically by (4.10). Phillips (1977, p. 190) suggests that C_p is about 0.23 for typical wind speeds. Use of the method used here yields the theoretical values for C_p shown in Fig. 6. Unrealistically small values for both C_p and the drag coefficient C_D are obtained if C_p is evaluated for a dominant wave with an amplitude given by the rms amplitude predicted by the Pierson–Moskowitz spectrum and a frequency equal to the peak frequency of the spectrum. This suggests that short waves play a large role in supporting the form drag, in accord with comments by Phillips and Wu.

We have also attempted to compare our results with Wu's laboratory measurements of flow over a progressive wave (Wu 1975), but have been frustrated by the anomalous behavior of Wu's drag coefficient, which decreases with increasing wind speed except for exceptionally strong winds. It appears necessary, therefore, to accept Wu's conclusion that his wind data has no general application because of the difference in scales between laboratory and field conditions. For wind speeds comparable to those encountered in typical oceanic conditions, the form drags computed using the present theory are considerably smaller than those measured by Wu, probably because, for the short waves observed by Wu, the form drag is unusually large owing to boundary layer separation in his experiments.

This is in accord with the results of our earlier paper, in which the growth rate of wind waves was predicted using the present model, and in which the theory was shown to agree reasonably well with Plant's empirical results (Plant 1982) for oceanic waves but to underestimate the growth rate for very short waves in a wave tank. It seems plausible, therefore, that boundary layer separation is a more important mechanism for inducing form drag in wave tanks than in oceanic waves, but that in both cases short waves contribute disproportionally to the pressure force on the surface.

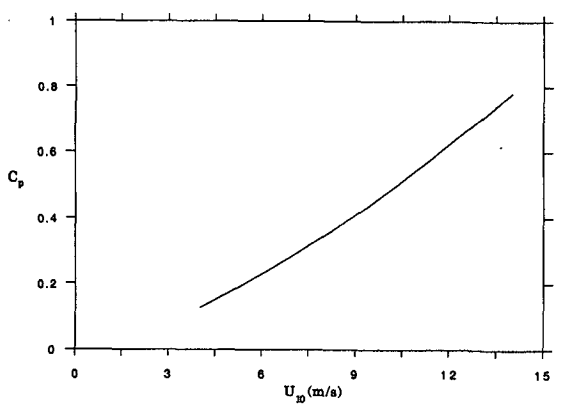

FIG. 6. Theoretical form drag coefficient C_p as function of U_{10}.

5. Discussion

The underlying premise of the present calculation is that form drag on a wavy surface can be attributed to a phase shift between the wave-induced pressure oscillation and the surface wave rather than to boundary layer separation, and can therefore be treated using standard boundary layer methods. As regards methodology, we have relied on the asymptotic results of our earlier paper and on the numerical calculations of Beljaars et al. in choosing a simple eddy viscosity model, since these studies indicate that there is little difference between such models in terms of their accuracy in calculating the surface pressure.

The good agreement noted earlier between our theoretical results and observations of the surface pressure for nonseparated flow serves to confirm the usefulness of the present method of turbulence modeling for treating flows of this type. However, the strong arguments made by Wu in his observational papers supporting the idea that boundary layer separation is the primary mechanism for form drag deserves further study, both in theories concerning the drag coefficient and in the closely related field of the generating mechanism for the growth of wind waves. Therefore, although the results of the present study appear to be consistent with measurements of the drag coefficient for flow over ocean waves, further observational work is needed to clarify the causes of the pressure force on the surface.

REFERENCES

Al-Zanaidy, M. A., and W. H. Hui, 1984: Turbulent airflow over water waves—a numerical study. *J. Fluid Mech.*, **148,** 225–246.

Beljaars, A. C. M., J. L. Walmsley and P. A. Taylor, 1987: A mixed spectral finite-difference model for neutrally stratified boundary-layer flow over roughness changes and topography. *Bound.-Layer Meteor.*, **38,** 273–303.

Cox, C., and W. H. Munk, 1954: Statistics of the sea surface derived from sun glitter. *J. Mar. Res.*, **13,** 198–227.

Dvoryaninov, G. S., and V. M. Zhuravlev, 1980: Toward a theory of the turbulent wave-mixing layer. *Izv., Acad. Sci. USSR, Atmos. Ocean. Phys.*, **16,** 422–428.

Garratt, J. R., 1977: Review of drag coefficients over oceans and continents. *Mon. Wea. Rev.*, **105,** 915–929.

Gent, P. R., and P. A. Taylor, 1976: A numerical model of air flow above water waves. *J. Fluid Mech.*, **77,** 105–128.

Jackson, P. S., and J. C. R. Hunt, 1975: Turbulent flow over a low hill. *Quart. J. Roy. Meteor. Soc.*, **101,** 929–955.

Jacobs, S. J., 1987: An asymptotic theory for the turbulent flow over a progressive water wave. *J. Fluid Mech.*, **174,** 69–80.

——, 1989: A pseudospectral method for two-point boundary value problems. *J. Comput. Phys.*, submitted.

Joseph, D., 1973: Domain perturbations: the higher order theory of infinitesimal water waves. *Arch. Rat. Mech. Anal.* **51,** 295–303.

Knight, D., 1977: Turbulent flow over a wavy boundary. *Bound.-Layer Meteor.*, **11,** 205–222.

Launder, B. E., G. J. Reece and W. Rodi, 1975: Progress in the development of a Reynolds stree turbulence closure. *J. Fluid Mech.*, **68,** 537–566.

McLean, J. W., 1983: Computation of turbulent flow over a moving wavy boundary. *Phys. Fluids,* **26,** 2065–2073.

Newley, T. M. J., 1985: Turbulent air flow over hills. PhD dissertation. University of Cambridge.

Olver, F. W. J., 1974: *Asymptotics and Special Functions.* Academic Press.

Perry, A. E., W. H. Schofield and P. N. Joubert, 1969: Rough wall turbulent boundary layers. *J. Fluid Mech.*, **37**, 383–413.

Phillips, O. M., 1977: *The Dynamics of the Upper Ocean,* 2nd ed. Cambridge University Press.

Plant, W. J., 1982: A relationship between wind stress and wave slope. *J. Geophys. Res.*, **87**, 1961–1967.

Schlichting, H., 1979: *Boundary Layer Theory,* 7th ed. McGraw-Hill.

Singhal, A. K., and D. B. Spalding, 1981: Predictions of two-dimensional boundary layers with the aid of the k-ϵ model of turbulence. Comput. Methods Appl. Mech. Eng., **25**, 365–383.

Sykes, R. I., 1980: An asymptotic theory of incompressible turbulent boundary-layer flow over a small hump. *J. Fluid Mech.*, **101**, 647–670.

Taylor, P. A., P. R. Gent and J. M. Keen, 1976: Some numerical solutions for turbulent boundary-layer flow above fixed, rough, wavy surfaces. *Geophys. J. Roy. Astron. Soc.*, **44**, 177–201.

Thorsness, C. B., P. E. Morrisroe and T. J. Hanratty, 1978: A comparison of linear theory with measurements of the variation of shear stress along a solid wave. *Chem. Eng. Sci.*, **33**, 579–592.

Van Dyke, M., 1975: *Perturbation Methods in Fluid Mechanics.* Parabolic Press.

Wu, J., 1975: Wind-induced drift currents. *J. Fluid Mech.*, **68**, 49–70.

——, 1980: Wind-stress coefficients over sea surface near neutral conditions—a revisit. *J. Phys. Oceanogr.*, **10**, 727–740.

Zilker, D. A., and T. J. Hanratty, 1979: Influence of the amplitude of a solid wavy wall on a turbulent flow. Part 2: Separated flows. *J. Fluid Mech.*, **90**, 257–271.

——, G. W. Cook and T. J. Hanratty, 1977: Influence of the amplitude of a solid wavy wall on a turbulent flow. Part 1: Non-separated flows. *J. Fluid Mech.*, **82**, 29–51.